JCTC Journal of Chemical Theory and Computation

Valence–Bond Order (VBO): A New Approach to Modeling Reactive Potential Energy Surfaces for Complex Systems, Materials, and Nanoparticles

Meiyu Zhao,[†] Mark A. Iron,[†,§] Przemysław Staszewski,[†,‡] Nathan E. Schultz,[†] Rosendo Valero,[†] and Donald G. Truhlar*[,†]

Department of Chemistry and Supercomputing Institute, University of Minnesota, Minneapolis, Minnesota 55455-0431, and Department of Theoretical Foundations of Biomedical Sciences and Medical Informatics, Collegium Medicum, Nicolaus Copernicus University, ul. Jagiellońska 13, 85-067 Bydgoszcz, Poland

Received October 28, 2008

Abstract: The extension of molecular mechanics to reactive systems, metals, and covalently bonded clusters with variable coordination numbers requires new functional forms beyond those popular for organic chemistry and biomolecules. Here we present a new scheme for reactive molecular mechanics, which is denoted as the valence–bond order model, for approximating reactive potential energy surfaces in large molecules, clusters, nanoparticles, solids, and other condensed-phase materials, especially those containing metals. The model is motivated by a moment approximation to tight binding molecular orbital theory, and we test how well one can approximate potential energy surfaces with a very simple functional form involving only interatomic distances with no explicit dependence on bond angles or dihedral angles. For large systems the computational requirements scale linearly with system size, and no diagonalizations or iterations are required; thus the method is well suited to large-scale simulations. The method is illustrated here by developing a force field for particles and solids composed of aluminum and hydrogen. The parameters were optimized against both interaction energies and relative interaction energies. The method performs well for pure aluminum clusters, nanoparticles, and bulk lattices and reasonably well for pure hydrogen clusters; the mean unsigned error per atom for the aluminum−hydrogen clusters is 0.1 eV/atom.

1. Introduction

The properties of molecules and materials result from internuclear (atomic) dynamics governed, in the Born−Oppenheimer approximation, by a potential energy surface that results from the system's electronic structure.[1] In principle, the electronic structure can be solved with high accuracy, and great progress has been made in accomplishing this for small molecules.[2,3] There are two general approaches for extending this progress to very large systems. The first is to derive simpler, yet sufficiently accurate, electronic structure methods. This includes theoretical advances in the description of electronic structure,[4−7] the development of semiempirical quantum mechanical electronic structure methods with reasonably reliable parametrizations,[8−13] and improved algorithms,[14−16] such as linear scaling methods.[17−19] The second general approach is to obtain analytic approximations to potential energy surfaces. If this is done for specific small systems,[20−22] additional work is needed to apply the treatment to extended systems. If this, however, can be done in terms of general parameters that are independent of the system size, then materials and large systems can be modeled without additional apparatus.

* To whom correspondence should be addressed. E-mail: truhlar@umn.edu.

[†] University of Minnesota.

[‡] Nicolaus Copernicus University.

[§] Current address: Computational Chemistry Unit, Department of Chemical Research Support, Weizmann Institute of Science, Rehovot, Israel 76100.

10.1021/ct8004535 CCC: $40.75
Published on Web 02/10/2009

Examples of such an approach include recent potential functions for a variety of materials,[23−31] including Al nanoparticles.[30,31]

Although traditional analytical potentials often have all their parameters fit to experiment, a more modern approach is to use high-level calculations. We note first that potentials fit only to properties of bulk metals or bulk materials containing metal atoms are unlikely to be accurate for defects, surfaces, nanostructured materials, or nanoparticles, but systematic data for these latter types of features or systems are scarce. However, many energetic properties that are not experimentally readily accessible can be calculated with reasonable accuracy. Even when measured values are available, it is sometimes hard to say whether a given measured value should be used in a fit, especially if the possible experimental error is greater than the desired accuracy of the computational method being parametrized. One recent example involved the heats of formation of the oxides and hydroxides of alkali and alkaline earth metals where widely different experimental values were obtained.[32] One main obstacle, however, to using calculated rather than experimental data is the difficulty in carrying out benchmark electronic structure calculations on subsystems that are large enough to represent the full complexity of the materials.

Analytic potentials are sometimes called classical potentials because they can be evaluated without recourse to the Schrödinger equation or other quantum formalisms. This is, however, a deceptive name for potentials fit to quantum mechanical electronic structure calculations.[31] If the fit is carefully done and the functional forms properly represent the physics, these potentials can capture the full quantum mechanical behavior of the potential energy surface within the Born−Oppenheimer approximation.

Great progress has been made in developing general parameters for analytic potentials for hydrocarbons, carbohydrates, biopolymers, and diverse organic compounds,[33−42] where this approach is traditionally termed molecular mechanics. Most molecular mechanics force fields are expressed in terms of local valence coordinates, specifically stretches, bends, and torsions, plus interatomic distances of nonbonded atoms. Since most molecular mechanics force fields do not describe bond breaking or bond rearrangement, they are restricted to nonreactive systems. Furthermore, they are easiest to parametrize for systems where the geometries are reasonably rigid and bonding types can be readily classified and catalogued, whereas valences of metal atoms are more variable, and bending and torsion parameters at metal−atom centers seem to be less transferable because the compounds are more flexible and bond lengths more variable than in organic chemistry. Thus very little progress has been made in extending this kind of force field to organometallic and inorganometallic systems, although Landis and Deeth and co-workers have attempted to incorporate some of this complexity for modeling organometallic complexes,[43,44] and Goddard and co-workers have suggested that a central force formalism, with local perturbations based on bond angles and torsions, may provide a useful starting point for both reactive and metal-containing systems, and they use this approach in their ReaxFF reactive force field.[25,27,29]

The goal of the present work is to present a new type of analytic function for modeling reactive and metal-containing systems and to test it for nanoparticles composed of aluminum and hydrogen. In recent years, we have been interested in designing potentials that can be used to describe and/or predict processes that occur in aluminum nanoparticles.[30,31,45] We developed two reasonably accurate potentials,[31] called NP-A and NP-B, for pure aluminum; NP-B is less accurate than NP-A but is much less expensive to evaluate and has been widely applied.[46−51] However, neither the NP-A nor the NP-B functional form is well suited for straightforward extension to heteronuclear systems.

A potential capable of describing metal hydride materials in both nanoparticles and the bulk would be of general interest. Hydrogen is potentially an important component of a clean energy storage medium, yet its transport, handling, and utilization involve a number of safety and technical problems. One possible strategy is to use metal hydrides as a storage medium.[52−63] Therefore, a potential energy function capable of accurately describing such a system would be useful.

In the present article we present a model called the valence–bond order (VBO) model. It provides a physically motivated starting point for representing the potential energy surfaces of both homonuclear and heteronuclear metal-containing and reactive systems. In Supporting Information we also present an extension called VBO2 as an illustration of an attempt to obtain better quantitative performance with a functional form motivated by VBO but more general. We illustrate VBO and VBO2 for particles composed of aluminum and hydrogen and for bulk aluminum, but the approach used here is also applicable to other metal hydride systems and to other materials and nanoparticles, although for some such more general applications it may be necessary to extend the functional form, for example, to include explicit Coulomb interactions, attractive noncovalent interactions, more complicated bond order terms, explicit bond angle or screening (three-body) terms, and so forth. Before considering such extensions, it is useful to learn how well the simple VBO form without such enhancements can represent potential energy functions, and the present paper provides a first answer to that question.

Section 2 presents the new formalism, section 3 presents the parametrization, and section 4 gives the results and characterizes the accuracy achievable with the method. Section 5 gives further discussion, especially of the relationship to other approaches.

2. Theory

2.1. Background. The key physical idea underlying the present approach is that the quantum mechanical nature of bonding manifests itself in the concepts of valence, bonding orbitals, and steric repulsion, all of which have a quantum mechanical basis ultimately rooted in the Pauli principle. These concepts are utilized, for example, in the valence-shell electron-pair repulsion (VSEPR) model[64,65] and the molecular orbital aufbau principle.[65,66] The most straightforward way to incorporate the effects of bonding orbitals

is to obtain the molecular orbitals by some variational or semiempirical method, which invariably involves diagonalizing a Hamiltonian matrix (such as a matrix representing a Fock or Kohn−Sham operator or some other effective one-electron Hamiltonian). Alternatively the quantum mechanical bonding effects can be included by valence bond theory,[1,65−71] which involves the diagonalization of a configuration interaction matrix. The difficulty in developing analytical potentials that do not require diagonalizations or an iterative process that is essentially equivalent to a diagonalization is in representing the saturation of bonding power (valence) of a given atom. Conventional molecular mechanics effectively accomplishes this by adopting a single-configuration valence bond formalism, where a different set of molecular mechanics parameters is associated with each bonding pattern, which in turn is associated with each valence bond configuration. This works well for nonreactive organic chemistry but requires a multiconfigurational extension[72,73] for reactions and is hard to extend to metals. Our approach presented here is different and is motivated instead by the second moment approximation to tight binding theory.

Tight-binding theory[9−11,13,74,75] may be justified[76−79] as an approximation to density functional theory, especially by using the noniterative formulation of Harris and Foulkes.[77−80] Tight-binding theory has been developed to simulate materials systems directly,[9−11,13,17,18,45,81−86] but it can also be further approximated to motivate analytic potentials. In particular, the closely related functional forms of the quasiatom theory,[87] the Gupta potential,[88] the embedded-atom model (EAM),[89] the modified EAM (MEAM),[90] the second-nearest-neighbor EAM (2NN-EAM),[91] the Finnis-Sinclair scheme,[92] the effective medium theory,[93] and the bond order potential[94] can all be motivated by the second moment approximation to tight binding theory.[95−105] These methods are closely related to each other, and they are also closely related to the Tersoff potential[106] and hence to the Brenner[23] and ReaxFF[25,27−29] potentials.[107] The relationship of EAM to the Pauling bond order has also been discussed.[108]

In the EAM and other closely related methods that we have mentioned, the energy is the sum of an attractive term that may be considered to approximate the cohesive band energy of tight-binding theory and a repulsive term representing mainly core−core repulsion. The cohesive term is proportional to the square root of the second moment of the density of states ($\sqrt{M}$), which may be approximated for each atom as the square root of a sum of two-body transfer integrals or the square root of the local coordination number. This idea is the basis for the functional form proposed here. In the basic version of the theory, to be called VBO (see below), unlike some earlier models, we retain only the simplest possible functional form, without added complications such as bond-angle terms and Coulombic terms. However, we generalize the square rooot, $\sqrt{M}$, to allow any fractional root, M^{ϕ}, where the fraction ϕ is positive and less than unity. This is motivated by a recognition that the value of one-half for ϕ is just one example of a more general principle of valence saturation, by which we mean that the bonding power of an atom for an additional ligand decreases as the number of ligands already bound increases. Other ways to motivate a value of ϕ other than one-half would be to consider the fourth root of the fourth moment (rather than the square root of the second moment) or to note that whereas the solution of a two-configuration bonding model, such as the London equation,[109] expresses valence saturation through a square root, a three-configuration model could involve a third root in the lowest eigenvalue.

In Supporting Information we present a second version, called VBO2, in which we include two cohesive terms for the homonuclear case and a third cohesive term for the heteronuclear case; we include explicit 3-body dependence for the heteronuclear case but still do not include explicit dependence on bond angles or coulomb forces. The VBO2 formulation involves two fractional powers rather than one; this may be justified either empirically (it sometimes gives more accurate results for a given number of parameters) or—more satisfactorily—by a two-band model.[110]

2.2. VBO. The new method presented here is called VBO. The first key element in the functional form is the bond order between atoms i and j, which is represented by a monotonically decreasing function of the distance r_{ij} between atoms i and j. A variety of such functions may be (and were) considered, but in the present work we present results only for the following cutoff decaying exponential function

$$b_{ij} = \begin{cases} N_{ij} \exp\left[\dfrac{-\gamma_{ij}}{1-(r_{ij}/\Delta_{ij})^{0.5}}\right] & \text{if } r_{ij} < \Delta_{ij} \\ 0 & \text{if } r_{ij} \geq \Delta_{ij} \end{cases} \quad (1)$$

where γ_{ij} and Δ_{ij} are parameters that depend on the atomic numbers of i and j. Notice that Δ_{ij} also plays the role of a cutoff value: as r_{ij} goes to Δ_{ij} from the left, b_{ij} goes to zero with an infinite number of continuous derivatives. N_{ij} is a normalization constant defined as

$$N_{ij} = \exp\left[\frac{\gamma_{ij}}{1-(R_{ij,0}/\Delta_{ij})^{0.5}}\right] \quad (2)$$

where $R_{ij,0}$ is the nominal bond distance of the ij dimer; the bond order of the dimer at this distance is defined to be unity. The factor N_{ij} and the constant $R_{ij,0}$ are included only for convenience of interpretation, and no energies depend on how the bond order is normalized because a different normalization would simply yield different optimized coefficients in expressions like eq 6.

The energy of the system is the sum of individual atomic contributions

$$E = \sum_i E_i \quad (3)$$

The form for E_i was inspired by the Morse potential[111] where the energy of a diatomic molecule is approximated as

$$E_{ij} = D_{ij}\{X_{ij}^2(r_{ij}) - 2X_{ij}(r_{ij})\} \quad (4)$$

where D_{ij} is a constant and

$$X_{ij} = \exp\left[-\alpha_{ij}(r_{ij} - R_{ij,0})\right] \quad (5)$$

and α_{ij} is another constant. Note that X_{ij} can be interpreted as the Pauling bond order.[112] In the VBO model, we replace

X_{ij} by b_{ij}, and we generalize eq 4 to a many-body system as follows

$$E_i = \sum_{j \neq i} (c_{i,1} b_{ij,1} + c_{i,2} b_{ij,2}) - V_i^{n_i} \quad (6)$$

where the valence V_i of atom i is defined by

$$V_i = \sum_{j \neq i} (c_{i,3} b_{ij,3} + c_{i,4} b_{ij,4}) \quad (7)$$

and b_{ij} has now become $b_{ij,p}$. Four different $b_{ij,p}$ functions with $p = 1, 2, 3, 4$, each with its own $\gamma_{ij,p}$ parameters, were used; $c_{i,p}$ (with $p = 1, 2, 3, 4$) and n_i are atomic parameters, whereas $\gamma_{ij,p}$ (with $p = 1, 2, 3, 4$) are parameters that depend on the atomic numbers of atoms i and j. All these parameters are positive by definition. Note that if $c_{i,2} = 0$, $c_{i,4} = 0$, and $n_i = 0.5$, then this functional has the same spirit as that used in the embedded atom[108] method but with a bond order function rather than an embedded density; furthermore, if one considers a diatomic molecule, uses eq 5 instead of eq 1 for the bond order, and sets $c_{i,2} = 0$, $c_{i,4} = 0$, $c_{i,3} = (2c_{i,1})^2$, and $n_i = 0.5$, one obtains a Morse[111] function. In eq 6, the last term is called the valence energy; this term is purely attractive, and the repulsive term is pairwise additive. The key physical constraint on the parameters of the VBO model is that n_i should be less than unity to account for valence saturation. But a key feature of the new method is that we will not constrain it to be exactly one-half, as in EAM.

The extension of the VBO model to a heteronuclear system such as a mixed aluminum−hydrogen system is more complicated than the way Hall combined two Morse potentials in order to map the potential energy surface for a collinear reaction.[113] Equation 4 is a quadratic function, and the simplest multinomial extension of such functions is to include cross-terms[113]

$$E_{ABC} = D_{AB}(X_{AB}^2 - 2X_{AB}) + D_{BC}(X_{BC}^2 - 2X_{BC}) + 2HX_{AB}X_{BC} \quad (8)$$

where H is a fitting parameter. But this cannot be applied to VBO because it does not show valence saturation in the same way. Therefore, we generalize VBO by replacing eq 7 by a more general valence expression, in particular

$$V_i = \sum_{j \neq i} (c_{i,3}\sigma_{ij,3} b_{ij,3} + c_{i,4}\sigma_{ij,4} b_{ij,4}) \quad (9)$$

In general the parameters depend on the atomic numbers of atoms i and j. When i and j have the same atomic numbers, we set $\sigma_{ij,3} = \sigma_{ij,4} = 1$ so that eq 9 reduces to eq 7 for homonuclear systems. In heteronuclear systems, $\sigma_{ij,p} \neq \sigma_{ji,p}$ if atoms i and j have different atomic numbers. The new parameters $\sigma_{ij,p}$ with $i \neq j$ allow the contribution of an Al atom to the valence of H to be different from the contribution of an H atom to the valence of Al. Similarly, $\gamma_{ij,p} \neq \gamma_{ji,p}$ for $p = 3$ or 4. However, the parameters $\gamma_{ij,p}$ for $p = 1$ or 2 are assumed invariant to permuting the order of the indices because these terms are pairwise additive. Equations 3, 6, and 9 define the VBO model.

2.3. Zero of Energy. The zero of energy is taken as the sum of the energies of the individual atoms at infinite separation. Thus all energies are interaction energies.

3. Determination of the Parameters

3.1. The Data Set. Three data sets, consisting of energies for specific geometries, were used: one each for pure aluminum, pure hydrogen, and mixed aluminum−hydrogen clusters.

For pure aluminum (Al_n clusters and nanoparticles), the data set, consisting of 808 structures calculated at either the PBE0[114]/6-311+G(3d2f)[115,116] (for $n \leq 13$) or PBE0[114]/MEC[117] (for $n > 13$) level, was taken from previous work.[31] The PBE0 functional was chosen based on comparison to high-level correlated wave function calculations on small clusters.[118] Data for bulk face-centered cubic (fcc), hexagonal close-packed (hcp), and body-centered cubic (bcc) quasi-spherical clusters data sets were also included, and they also were taken from previous work.[31]

For pure hydrogen, part of the data set was also taken from the literature: 80 H_2 points from the accurate calculations by Kołos and Wolniewicz,[119] 602 H_3 points (307 C_{2v}, 22 $D_{\infty h}$, 21 D_{3h}, and 252 $C_{\infty v}$) determined using the BKMP2 H_3 potential energy surface of Boothroyd et al.,[120] and 586 H_4 points (279 for parallel approach of two H_2 molecule, 307 for perpendicular approach of two H_2 molecules) determined using the BMKP H_4 potential energy surface of Boothroyd et al.[121]

In addition to these data for H_2, H_3, and H_4, we generated new data for H_6 and H_8 by performing high-level ab initio calculations at selected geometries. Because H atoms do not form extended systems, except for condensed-phase H_2, in contrast to aluminum atoms, which can form nanoparticle and bulk aluminum phases, pure hydrogen clusters with more than 8 atoms are not considered here.

Two types of H_6 structures were included in the data set. To construct the first type, the saddle point of the H + H_2 reaction was optimized at the UHF[122]/cc-pVTZ[123] level of theory, and two identical collinear H_3 fragments in this geometry were used to form an H_6 fragment, with the second H_3 fragment pointing toward the central atom of the first H_3 fragment. The six H_6 geometries included in the data set have closest distances between the two H_3 fragments varying between 0.7 and 1.2 Å. The second type of H_6 structure was constructed starting with a configuration analogous to that of the CH_5^+ cation, which on optimization leads to a structure of the type H_4 + H_2. In the six structures included in the data set, the distance between the H_4 and H_2 fragments was varied between 0.82 and 1.23 Å.

The H_8 data set is also composed of two types of structures. The first type has two square H_4 fragments situated side-by-side, where the H−H distances in the H_4 fragments were previously optimized. Then, six points were generated by varying the distance between the H_4 fragments from 0.46 and 0.80 Å. The second type of H_8 structure derives from an ethane-like configuration for the hydrogen atoms. The optimized structure has a long H−H central distance with each of the two H atoms involved being attached to three H atoms. Six points were added to the data set with the central distance ranging from 1.25 to 1.97 Å.

The electronic energies of the H_6 and H_8 structures were obtained from extrapolated multireference configuration

interaction[124] (MRCI) calculations with a quadruples correction[125] (+Q). First, full-CI (FCI) calculations were performed for H_6 and H_8 with a double-ζ basis set with two goals: (1) to determine whether the singlet, triplet, or quintet is the lowest-energy spin state for the given structure, and (2) to establish a benchmark on which to base the choice for the reference space in the MRCI calculations. In this way, it was determined that the H_6 and H_8 structures have triplet and singlet ground states, respectively. To determine the complete active space self-consistent field[126,127] (CASSCF) reference state in the MRCI calculations, the H_3 and H_4 energies were calculated at the FCI level. Complete active spaces of 3 electrons in 6 orbitals, denoted (3,6), and 4 electrons in 6 orbitals, denoted (4,6), were chosen as the MRCI reference spaces for H_3 and H_4, respectively, and provided a maximum error of about 0.1 kcal/mol with respect to the FCI results. Thus, (6,12) and (8,12) reference spaces were chosen for the H_6 and H_8 calculations.

The final electronic energies for the H_6 and H_8 structures were obtained using the following form[128] of basis-set extrapolation

$$E_\infty^{\mathrm{tot}} = \frac{3^\alpha}{3^\alpha - 2^\alpha} E_3^{\mathrm{CASSCF}} - \frac{2^\alpha}{3^\alpha - 2^\alpha} E_2^{\mathrm{CASSCF}} + \frac{3^\beta}{3^\beta - 2^\beta} E_3^{(\mathrm{MRCI+Q})-\mathrm{CASSCF}} - \frac{2^\beta}{3^\beta - 2^\beta} E_2^{(\mathrm{MRCI+Q})-\mathrm{CASSCF}} \quad (10)$$

where E_2 and E_3 are energies obtained using the cc-pVDZ and cc-pVTZ basis sets, respectively, and MRCI+Q denotes multireference CI with singles and doubles and Pople's correction for quadruples; the parameters α and β were taken to have the values[128] 3.4 and 2.4, respectively.

The pure hydrogen data set for H_2, H_3, and H_4 consists of 1268 data, and adding the H_6 and H_8 data increases this to 1292 data; the resulting data set is called the H1292 database. The data set of mixed aluminum−hydrogen particles consists of 906 Al_nH_m geometries ($n = 1-13$, $m = 1-12$) and energies calculated at the PBE0/6-311++G(3d2f,2p) level of theory and is called the AlH906 database.

We also considered bulk data for pure aluminum. The accurate cohesive energies for fcc, bcc, and hcp lattices with given lattice constants were estimated in ref 31, and those data are also used here. To calculate bulk cohesive energies for a given lattice constant from the model potentials, we used the procedure of ref 31 where the bulk cohesive energy is defined as the energy per atom required to atomize a particle, extrapolated to an infinitely large particle from finite-size fcc, bcc, and hcp quasispherical particles with given nearest-neighbor distances corresponding to the lattice constants for which accurate data are available.

All geometries and energies used in fitting are provided in Supporting Information.

3.2. The Optimization of Parameters. A microgenetic algorithm[129] was used to fit the parameters. In particular, we used the FORTRAN version 1.7a of Carroll's code,[130] locally modified with our own fitness function and designed to run in parallel using the message-passing interface (MPI).[131,132]

The fitness function used here is based on the fitness functions used in previous work[31,45] to parametrize analytical functions and tight-binding models. In each case, the data sets are divided into subgroups (with n_k particles in subgroup k) according to the size of the particles, i.e., the number of atoms N_i in each particle i and their stoichiometry. Thus, for example, although Al_4H and AlH_4 clusters both have $N_i = 5$; they are in different subgroups, but, as previously,[31] some subgroups for pure aluminum contain more than one N_i. Note that we use "particle" as a generic name for either a "cluster" (which is arbitrarily defined to have less than 20 Al atoms) or a "nanoparticle" (which is correspondingly defined to have 20 or more Al atoms).

For pure Al, there are 11 groups with $N_i = 2$ in group $k = 1$, $N_i = 3$ in group $k = 2$, up to $N_i = 89-177$ in group $k = 11$.[31] The sum of the n_k for pure Al is 808. For hydrogen particles, there are five subgroups, each with a single value (2, 3, 4, 6, or 8) of N_i. For heteronuclear particles each

Table 1. VBO Parameters for Pure Al and Pure H

parameter (units)	Al	H
$\gamma_{ij,1}$	0.3599	2.7292
$\gamma_{ij,2}$	4.2538	8.8100
$\gamma_{ij,3}$	0.5684	16.1462
$\gamma_{ij,4}$	2.9562	16.1330
$c_{i,1}$ (eV)	0.2248	2.0112
$c_{i,2}$ (eV)	0.2172	0.8084
$c_{i,3}$ (E_h^{1/n_j})[a]	0.0133	0.00001
$c_{i,4}$ (E_h^{1/n_j})[a]	0.0068	0.00001
n_i	0.7931	0.1536
$R_{ij,0}$ (Å)	2.7306[b]	0.7414[b]

[a] E_h denotes one hartree, that is, one atomic unit of energy. [b] As explained in the text, this is not a fitting parameter; it simply gives the bond order a convenient ("physical") normalization.

Table 2. VBO Parameters for Al−H Interactions

parameter	Al−H	parameter	Al−H
$\gamma_{HAl,1}$	7.4891	$\sigma_{HAl,4}$	0.0191
$\gamma_{HAl,2}$	1.8993	$\sigma_{AlH,3}$	2.9306
$\gamma_{HAl,3}$	13.5669	$\sigma_{AlH,4}$	0.00008
$\gamma_{HAl,4}$	13.6902	$c_{HAl,1}$ (eV)	0.3509
$\gamma_{AlH,3}$	1.6911	$c_{HAl,2}$ (eV)	0.5174
$\gamma_{AlH,4}$	2.8674	$R_{ij,0}$[a] (Å)	1.6637
$\sigma_{HAl,3}$	0.00001		

[a] As explained in the text, this is not a fitting parameter; it simply gives the bond order a physical normalzation.

Table 3. Mean Unsigned Errors (in eV/atom) for Aluminum

method (model)	ε_{bulk}	ε_{CE}	ε_{part}	$\varepsilon_{cluster}$[a]	ε_{nano}[b]
VBO	0.02	0.002	0.05	0.06	0.03
NP-A[c]	0.02	0.002	0.05	0.06	0.03
NP-B[c]	0.03	0.002	0.06	0.08	0.04

[a] MUE for cluster with 2−19 atoms. [b] MUE for nanoparticles with 20−177 atoms. [c] Reference 31.

Table 4. Bulk Lattice Constants (LC, in Ångstroms) and Bulk Cohesive Energies (E_c in eV/atom) for Aluminum

	fcc		bcc		hcp	
method (model)	LC	E_c	LC	E_c	LC	E_c
accurate[a]	4.02	3.43	3.24	3.33	2.87	3.39
VBO	4.02	3.44	3.22	3.25	2.85	3.49
NP-A[a]	4.01	3.43	3.22	3.34	2.84	3.42
NP-B[a]	4.03	3.43	3.27	3.35	2.86	3.41

[a] Reference 31.

subgroup k has a unique combination of N_i and stoichiometry. Thus for pure hydrogen and heteronuclear systems, we introduce the notation N_k for the N_i value of subgroup k.

We consider errors on a per-atom basis so that errors in the larger clusters do not dominate our considerations simply because of the size of the larger clusters. (The per-atom convention is standard in discussing cohesive energy of bulk materials.) We define a mean unsigned error (MUE) per atom for subgroup k as

$$\varepsilon_k = \frac{1}{2}\left(\frac{\sum_{i=1}^{n_k} w_i \Delta E_i^k}{\sum_{i=1}^{n_k} w_i} + \frac{\sum_{i=1}^{n_k-1}\sum_{j=i+1}^{n_k} w_i w_j \delta_{N_i N_j} \Delta\Delta E_{ij}^k}{\sum_{i=1}^{n_k-1}\sum_{j=i+1}^{n_k} w_i w_j \delta_{N_i N_j}} \right) \quad (11)$$

where w_i is the weight of particle i, and $\delta_{N_i N_j}$ is a Kronecker delta. For pure aluminum, the form of w_i is the same as eq 1 of ref 31. For pure hydrogen and mixed aluminum−hydrogen particles, $w_i = 1$. In eq 11, the quantity ΔE_i^k is the difference between the accurate (acc) and the VBO energies (each relative to separated atoms) for structure i of subgroup k

$$\Delta E_i^k = (E_i^{k,\mathrm{acc}} - E_i^{k,\mathrm{VBO}})/N_i \quad (12)$$

and $\Delta\Delta E_{ij}^k$ is defined by

$$\Delta\Delta E_{ij}^k = (\Delta E_i^k - \Delta E_j^k)/N_i \quad (13)$$

Thus ΔE_i^k is a measure of the error in absolute interatomic interaction energy on a per atom basis for a given geometry, whereas $\Delta\Delta E_{ij}^k$ is a measure, again on a per atom basis, of the accuracy of relative binding energies, that is, of the shape of the potential energy surface. The importance of including $\Delta\Delta E_{ij}^k$ was demonstrated previously.[13,30]

For pure Al we computed a mean unsigned error for all particles by

$$\varepsilon_{\mathrm{part}} = \left(\sum_{k=1}^{N_s} \varepsilon_k \right)/N_s \quad (14)$$

where N_s is the number of subgroups (11 for pure Al). For pure Al, we also compute $\varepsilon_{\mathrm{cluster}}$ in which eq 14 is applied only to the six subgroups with $N_i \leq 19$ and $\varepsilon_{\mathrm{nano}}$ in which eq 14 is applied only to the five subgroups with $N_i \geq 20$. For hydrogen we used eq 14 with $N_s = 3$ (see below). For mixed aluminum−hydrogen particles, we used

$$\varepsilon_{\mathrm{part}} = \frac{\sum_k n_k^\alpha N_k^\beta \varepsilon_{N_k}}{\sum_k n_k^\alpha N_k^\beta} \quad (15)$$

with $\alpha = 0.4$ and $\beta = 0.6$.

Since a genetic algorithm is used to maximize a function, but our goal is to minimize the total error ε, the fitness function f is defined as

$$f = -\varepsilon \quad (16)$$

where ε is the error to be minimized. For hydrogen and heteronuclear hydrogen−aluminum particles, we set ε equal to $\varepsilon_{\mathrm{part}}$. For pure aluminum, we used[31]

$$\varepsilon = \frac{1}{4}(\varepsilon_{\mathrm{bulk}} + \varepsilon_{\mathrm{CE}}) + \frac{1}{2}\varepsilon_{\mathrm{part}} \quad (17)$$

where $\varepsilon_{\mathrm{bulk}}$ and $\varepsilon_{\mathrm{CE}}$ are, respectively, the errors in the bulk energies and in the FCC cohesive energies. In eq 17, $\varepsilon_{\mathrm{bulk}}$ is the average unsigned error over 12 energetic data for fcc, bcc, and hcp as in ref 31 (we considered four lattice constants for each crystal habit), whereas $\varepsilon_{\mathrm{CE}}$ is for the subset of four data four fcc.

3.3. Parameterization. In eq 1, the parameter Δ_{ij} acts as a cutoff distance for the bond order. In previous work[31] on pure Al, we used a similar cutoff, with values of 6.50 Å for our best potential, called NP-A, and 5.38 Å for a second potential, called NP-B, that was slightly less accurate but much more economical. The calculation times for large particles increase with increasing Δ_{ij} and the onset of linear scaling is pushed up to larger nanoparticles. Therefore, in all further work, Δ_{ij} was frozen somewhat arbitrarily at 6.88 Å for Al−Al and Al−H interactions and at 5.29 Å for H−H interactions.

A more commonly used approximation for the bond order is Pauling's approximation,[112] which is a simple exponential function as in eq 5. We found that replacing b_{ij} with a simple exponential did not significantly improve the results, and so we retained the cutoff bond order of eq 1 for the present parametrization.

There are nine free parameters in the VBO model for pure aluminum and nine for pure hydrogen. We first optimized the parameters for pure Al and pure H. VBO did not yield satisfactory results for H_6 and H_8, so we excluded them from the final optimization. The final values of the VBO parameters and $R_{ij,0}$ for Al−Al and H−H interactions are listed in Table 1. The optimized values of n_i are less than one; this physically corresponds to valence saturation as the bond order increases.

When optimizing the heteronuclear parameters, we froze the Al−Al and H−H parameters at the values already found for the pure systems. The number of heteronuclear parameters for Al−H systems is 12 in VBO. In the initial stages of optimization all parameters were optimized, and the importance of various parameters was examined. No terms were dropped, and the final heteronuclear parameters are given in Table 2.

4. Results

For pure aluminum, the mean unsigned errors for VBO are given in Table 3. Table 3 shows that for aluminum particles VBO performs as well as the much more expensive NP-A, which contains two three-body terms, and better than the less expensive embedded-atom-based NP-B, which includes

Table 5. MUEs (eV/atom) for Pure Hydrogen[a]

K	1	2	3	$\varepsilon_{\mathrm{part}}$
formula	H_2	H_3	H_4	
N_k	2	3	4	
n_k	80	602	586	
VBO	0.02	0.06	0.14	0.07

[a] In Tables 5 and 6, the last row gives the MUE per atom for the n_k data subgroup k, where subgroup k contains particles with N_k atoms, except in the last column where the last row gives ϵ_{part}.

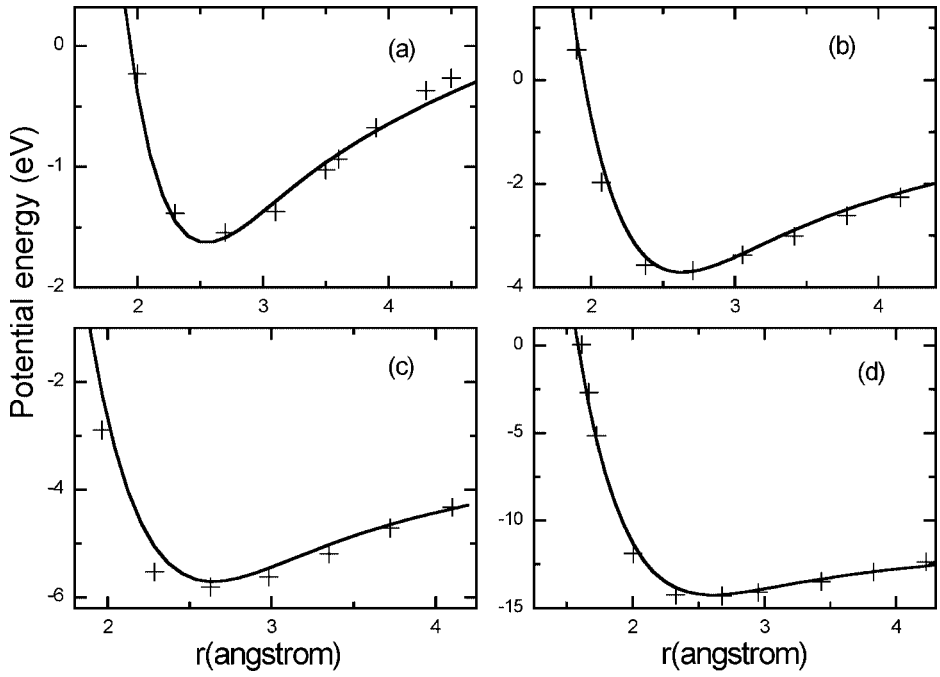

Figure 1. Potential energies of aluminum clusters as calculated by the VBO method (solid curves) as compared to PBE0/6-311+G(3d2f) reference data (crosses): (a) Al_2 dimer, (b) Al_3 for the sideways approach of Al to the dimer with a dimer bond length of 2.8635 Å, (c) Al_4 for the planar, short-bridge approach of Al to Al_3 (for this plot, Al_3 is an acute isosceles triangle with the short bond being the base of length 2.54724 Å and the height being 2.20598 Å, and the fourth Al approaches the short bond along the C_2 axis), and (d) Al_7 for the approach of Al to a 3-fold face of a regular octahedron with bond length 2.6634 Å. In all plots, r is the distance between the approaching Al atom and the closest Al atom in the approached subcluster.

Table 6. MUEs (eV/atom) for Heteronuclear Particles Composed of Aluminum and Hydrogen

k	1	2	3	4	5	6	7	8	9	10	11	12	13	14	15	ε_{part}
formula	AlH	AlH_2	AlH_3	AlH_4	AlH_5	AlH_6	AlH_{12}	Al_2H	Al_2H_2	Al_3H	Al_4H	$Al_{13}H$	$Al_{13}H_2$	$Al_{13}H_8$	$Al_{13}H_{12}$	
N_k	2	3	4	5	6	7	13	3	4	4	5	14	15	21	25	
n_k	37	108	54	3	3	3	3	304	3	74	180	125	3	3	3	
VBO	0.05	0.14	0.33	0.05	0.10	0.30	0.35	0.06	0.16	0.08	0.11	0.03	0.05	0.06	0.08	0.11

three-body effects through the use of an embedding function rather than by explicit three-body terms. Figure 1 shows four cuts through the potential surfaces for various sizes of clusters (these plots are similar to plots in previous papers[13,118] on Al clusters; the geometries used for these cuts are specified qualitatively in words in the figure captions and precisely by tables of geometries and energies in Supporting Information). The figure shows that VBO not only gives small mean unsigned errors, it also reproduces the shapes of the potential energy curves.

Table 4 shows that VBO also reproduces the bulk aluminum cohesive energy and lattice constants semiquantitatively.

Mean unsigned errors for pure hydrogen are given in Table 5. The average error for hydrogen is 0.07 eV/atom for VBO, which is the same order of magnitude as for aluminum, but a little larger.

MUEs for heteronuclear aluminum−hydrogen particles are given in Table 6. The number n_k of particles in each subgroup is also included in the table. The maximum MUE per atom is 0.35 eV, which is the MUE for the AlH_{12} cluster. The minimum MUE per atom is 0.03 eV/atom for the $Al_{13}H$ cluster. Most of the MUEs are in the range of 0.03−0.16 eV/atom. The overall error is 0.11 eV/atom, which is about twice as large as $\epsilon_{cluster}$ for pure Al. Figure 2 shows four cuts through the potential energy surfaces for mixed aluminum−hydrogen clusters (the geometries used in these cuts are specified qualitatively in words in the figure captions and precisely by tables of geometries and energies in Supporting Information); as for pure aluminum we see that the VBO model represents the qualitative dependence of the energy on structure quite well. The local maximum in Figure 2d corresponds to the passage of H through a triangular face between the exterior of the cluster and an interstitial site; VBO does quite well for reproducing this potential energy curve.

5. Discussion

Methods for calculating potential energy functions may be divided into those in which electrons are treated explicitly, for example, coupled cluster theory,[2,3] density functional theory,[4,5] or semiempirical molecular orbital theory[8−13] (including tight binding theory[9−11,13]), or those in which electrons are only implicit; a generic name for the latter is molecular mechanics.[33−42,133] As mentioned in the introduction, the molecular mechanics method usually yields analytic potential functions with general parameters designed to be transferable between systems (as opposed, for example, to potentials designed for a specific system, such as the water dimer[21] or the reaction of H with CH_4[22]). The set of general parameters is sometimes called

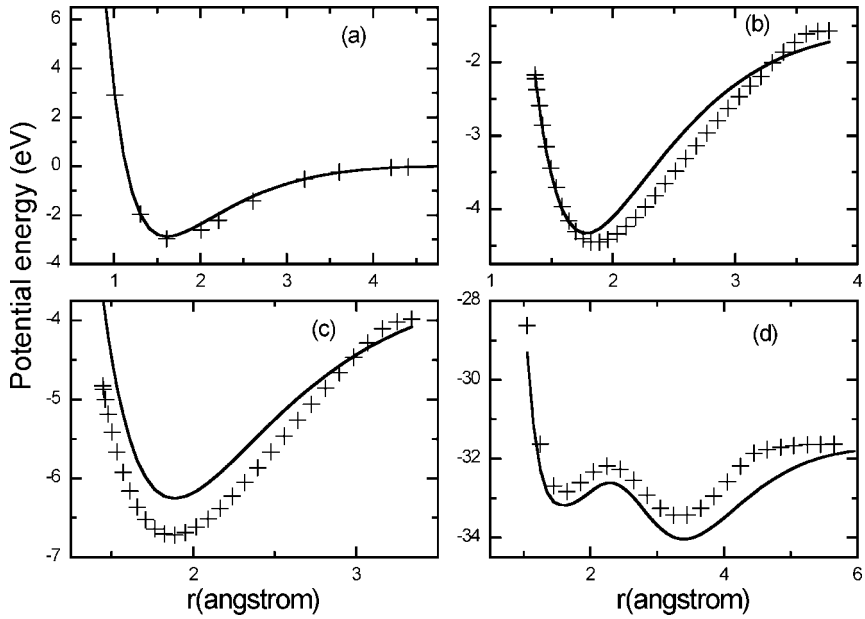

Figure 2. Potential energies of aluminum−hydrogen mixed clusters calculated by the VBO method (solid curves) as compared to PBE0/6-311++G (3d2f,2p) reference data (crosses): (a) AlH dimer, (b) Al_2H for the sideways approach of H to the Al_2 dimer with an Al−Al bond distance of 2.73 Å, (c) Al_3H for the 3-fold approach of H to an Al_3 triangle (for this plot, Al_3 is an equilateral triangle with the a bond length equal to 2.50696 Å, and the H approaches its center along the C_3 axis), and (d) approach of H to Al_{13} cluster (FCC structure) toward a 3-fold site but with C_1 symmetry. In all plots, r is the distance between the approaching H atom and an Al atom in the approached subcluster.

a force field,[37−42] although literally that term should refer to the gradient field of the potential energy function for a specific system.

As mentioned in the introduction, many molecular mechanics force fields (conventional molecular mechanics) are designed for treating only nonreactive systems or reactive systems for geometries in the neighborhoods of equilibrium geometries,[33−42,133] although there are some notable exceptions such as the Tersoff potential for systems composed of Si and C or Ge,[106] the Brenner potentials for hydrocarbons,[23] the Streitz−Mintmire potential for systems composed of Al and O,[24] and the ReaxFF force fields for a variety of materials, including hydrocarbons[25] and materials composed of Si and O,[27] Al and O,[28] or Mg and H.[29] These exceptions maybe called reactive molecular mechanics. VBO is designed as a form of reactive molecular mechanics, and in this article we presented a general parametrization for systems composed of Al and H.

A key difference between the reactive molecular mechanics force fields[23−29,107] and the conventional nonreactive ones[33−42,133] is the absence of typing in reactive force fields. In conventional molecular mechanics one specifies the type and bonding arrangement for each atom, e.g., an O might be typed as sp^3, and the user of the force field specifies the two atoms to which it is bonded. In reactive force fields, an atom interacts with all other atoms, except possibly for a smooth cutoff based solely on distance, and the parameters are the same for every Al, or every O, or every H independent of any perceived bonding pattern in a given geometry. Furthermore, the bonding interactions yield physically correct results when bonds break, as in a Morse potential,[111] as contrasted to harmonic or other polynomial interactions often used in conventional molecular mechanics.

For ionic or charged systems or systems whose bonds have large partial ionic character, one should include explicit Coulomb interactions in the functional form.[2,4,25,27−29,34,36−42] Al and H have different electronegativity values, but the difference corresponds to only about 10% partial ionic character[112a] (as compared to about 20% for Mg−H and 30% for Al−O). Therefore, at least for now, we omitted explicit Coulombic terms. Another key issue is whether to include explicit angle-dependent terms.[23,25,27,29,33,4,106,134] Similarly to deciding not to include Coulombic terms, at least for the present, we attempted here to see how well the VBO form can work without angle-dependent terms.

These choices led us to a very simple functional form, much simpler than any of those mentioned above, and the present results are encouraging in that this simple functional form already provides a qualitatively correct description of aluminum-hydrogen clusters with a wide range of compositions (wide range of Al-to-H ratios in the clusters). This kind of analytic potential energy function is therefore well suited to the largest simulations, such as long-time simulations of the dynamics of large nanoparticles, ceramics, or polycrystalline materials.[135,136] A second possible use for low-cost potential energy functions with general parameters is as a starting point for a more accurate potential energy function for a specific system or reaction; for example, sometimes one starts with a general parametrization and then introduces specific reaction parameters.[137−140] For a more specific example, one might reoptimize the general parameters for diffusion of a single hydrogen atom in bulk Al or to treat a system of two hydrogen atoms interacting with Al_{13} or with a specific crystal face of solid Al. By focusing on a less diverse set of structures, one can obtain a much more accurate potential energy surface.

One goal of the present work has been to test the accuracy attainable within a VBO scheme without explicit dependence on bond angles. The primitive VBO scheme employs one

valence per atom and involves only radial two-body forces. The VBO2 scheme presented in Supporting Information involves two or three valences per atom and includes two-body homonuclear and heteronuclear radial forces and three-body heteronuclear forces; the latter implicitly bring in bond angle dependences. Directions for further study include three-body homonuclear forces, four-body forces, explicit dependence on bond angles or dihedral angles, and explicit accounting for Coulomb and dispersion interactions.

6. Conclusion

The VBO method has been proposed and developed for modeling a metal hydride system. The VBO model should be applicable to many other pure and binary materials as well, and there is no reason why it cannot be extended to ternary or other multicomponent systems. Here the model was used to develop a force field for nanoparticles composed of aluminum and hydrogen. The overall error is just 0.11 eV/atom on average for heteronuclear systems and 0.05−0.07 eV/atom for homonuclear systems. In Supporting Information we illustrate how the VBO functional form can be used as a starting point for functional forms with more parameters and flexibility. In particular, we present an extension called VBO2 and show that it is more accurate for pure hydrogen clusters and slightly more accurate for mixed aluminum−hydrogen clusters.

The computational expense of VBO scales linearly with system size, and diagonalization or iterations are not required; the method is therefore particularly useful for simulating large systems.

Acknowledgment. The authors are grateful to Ahren Jasper for helpful assistance and to Steven Mielke, Steve Valone, Akin Budi, Julian Gale, David Henry, and Irene Yarovsky for helpful comments. This work was supported in part by the National Science Foundation under Grant Nos. ITR-0428774 and CHE-0704974.

Supporting Information Available: Equations and results for the VBO2 model; geometries and energies (relative to separated atoms) for all data in the training set. This material is available free of charge via the Internet at http://pubs.acs.org.

References

(1) Slater, J. C. *Quantum Theory of Matter*, 2nd ed.; McGraw-Hill: New York, NY, 1968.

(2) Raghavachari, K.; Anderson, J. B. *J. Phys. Chem.* **1996**, *100*, 12960.

(3) Pople, J. A. *Rev. Mod. Phys.* **1999**, *71*, 1267.

(4) Kohn, W.; Becke, A. D.; Parr, R. G. *J. Phys. Chem.* **1996**, *100*, 12974.

(5) Kohn, W. *Rev. Mod. Phys.* **1999**, *71*, 1253.

(6) Truhlar, D. G. In *Foundations of Molecular Modeling and Simulation*; Cummings, P. T., Westmoreland, P. R., Eds.; American Institute of Chemical Engineers: New York, NY, 2001; pp 71−83.

(7) Friesner, R. A. *Proc. Natl. Acad. Sci. U.S.A.* **2005**, *102*, 6648.

(8) Zerner, M. C. *Rev. Comput. Chem.* **1991**, *2*, 313.

(9) Wang, C. Z.; Ho, K. M. *J. Comput.-Aided Mater. Des.* **1996**, *3*, 139.

(10) *Tight-Binding Approach to Computational Materials Science*; Turchi, P. E. A.; Gonis, A.; Colombo, L., Eds.; Materials Research Society: Warrendale, PA, 1998.

(11) Frauenheim, T.; Seifert, G.; Elstner, M.; Niehaus, T.; Kohler, C.; Amkreutz, M.; Sternberg, M.; Hajnal, Z.; Di Carlo, A.; Suhai, S. *J. Phys.: Condens. Matter* **2002**, *14*, 3015.

(12) Bredow, T.; Jug, K. *Theor. Chem. Acc.* **2005**, *113*, 1.

(13) (a) Staszewska, G.; Staszewski, P.; Schultz, N. E.; Truhlar, D. G. *Phys. Rev. B* **2005**, *71*, 045423. (b) Iron, M. A.; Heyden, A.; Staszewska, G.; Truhlar, D. G. *J. Chem. Theory Comp.* **2008**, *4*, 804.

(14) *Quantum Simulations of Complex Many-Body Systems: From Theory to Algorithms*; Grotendorst, J., Marx, D., Muramatsu, A., Eds.; Neumann Institute for Computing: Julich, 2002.

(15) *Multiscale Computational Methods in Chemistry and Physics*; Brandt, A.; Bernholc, J.; Binder, K., Eds.; IOS Press: Amsterdam, 2001.

(16) Hill, J.-R.; Subramanian, L.; Maiti, A. *Molecular Modeling Techniques in Material Sciences*; Taylor and Francis Group: Boca Raton, FL, 2003.

(17) Qiu, S. Y.; Wang, C. Z.; Ho, K. M.; Chan, C. T. *J. Phys.: Condens. Matter* **1994**, *6*, 9153.

(18) Goedecker, S.; Colombo, L. *Phys. Rev. Lett.* **1994**, *73*, 122.

(19) Nam, K.; Gao, J. L.; York, D. M. *J. Chem. Theory Comput.* **2005**, *1*, 2.

(20) Truhlar, D. G.; Steckler, R.; Gordon, M. S. *Chem. Rev.* **1987**, *87*, 217.

(21) Huang, X. C.; Braams, B. J.; Bowman, J. M. *J. Phys. Chem. A* **2006**, *110*, 445.

(22) Albu, T. V.; Espinosa-Garcia, J.; Truhlar, D. G. *Chem. Rev.* **2007**, *107*, 5101.

(23) Brenner, D. W. *Phys. Rev. B* **1990**, *42*, 9458.

(24) Streitz, F. H.; Mintmire, J. W. *Phys. Rev. B* **1994**, *50*, 11996.

(25) van Duin, A. C. T.; Dasgupta, S.; Lorant, F.; Goddard, W. A. *J. Phys. Chem. A* **2001**, *105*, 9396.

(26) (a) Bazant, M. Z.; Kaxiras, E. *Phys. Rev. Lett.* **1996**, *77*, 4370. (b) Bazant, M. Z.; Kaxiras, E.; Justo, J. F. *Phys. Rev. B* **1997**, *56*, 8542. (c) Justo, J. F.; Bazant, M. Z.; Kaxiras, E.; Bulatov, V. V.; Yip, S. *Phys. Rev. B* **1998**, *58*, 2539. (d) Stuart, S. J.; Tuten, A. B.; Harrison, J. A. *J. Chem. Phys.* **2000**, *112*, 6472. (e) Marks, N. A. *Phys. Rev. B* **2001**, *63*, 035401. (f) Brenner, D. W.; Shenderova, O. A.; Harrison, J. A.; Stuart, S. J.; Ni, B.; Sinnott, S. B. *J. Phys.: Condens. Matter* **2002**, *14*, 7–83. (g) Brenner, D. W.; Shenderova, O. A.; Areshkin, D. A.; Schall, J. D.; Frankland, S. J. V. *Comput. Mod. Eng. Sci.* **2002**, *3*, 643. (h) Ni, B.; Lee, K.-H.; Sinnott, S. B. *J. Phys.: Condens. Matter* **2004**, *I*, 7261. (i) Shi, Y.; Brenner, D. W. *J. Chem. Phys.* **2007**, *127*, 134503.

(27) van Duin, A. C. T.; Strachan, A.; Stewman, S.; Zhang, Q. S.; Xu, X.; Goddard, W. A. *J. Phys. Chem. A* **2003**, *107*, 3803.

(28) Zhang, Q.; Cagin, T.; van Duin, A.; Goddard, W. A.; Qi, Y.; Hector, L. G. *Phys. Rev. B* **2004**, *69*, 045423.

(29) Cheung, S.; Deng, W. Q.; van Duin, A. C. T.; Goddard, W. A. *J. Phys. Chem. A* **2005**, *109*, 851.

(30) Jasper, A. W.; Staszewski, P.; Staszewska, G.; Schultz, N. E.; Truhlar, D. G. *J. Phys. Chem. B* **2004**, *108*, 8996.

(31) Jasper, A. W.; Schultz, N. E.; Truhlar, D. G. *J. Phys. Chem. B* **2005**, *109*, 3915.

(32) Sullivan, M. B.; Iron, M. A.; Redfern, P. C.; Martin, J. M. L.; Curtiss, L. A.; Radom, L. *J. Phys. Chem. A* **2003**, *107*, 5617.

(33) Bowen, J. P.; Allinger, N. L. *Rev. Comput. Chem.* **1991**, *2*, 81.

(34) Cornell, W. D.; Cieplak, P.; Bayly, C. I.; Gould, I. R., Jr.; Ferguson, D. M.; Spellmeyer, D. C.; Fox, T.; Caldwell, J. W.; Kollman, P. A. *J. Am. Chem. Soc.* **1995**, *117*, 5179.

(35) Allinger, N. L.; Chen, K.; Lii, J.-H. *J. Comput. Chem.* **1996**, *17*, 642.

(36) Halgren, T. A. *J. Comput. Chem.* **1996**, *17*, 490.

(37) MacKerrell, A. D., Jr.; Bashford, D.; Bellott, M.; Dunbrack, R. L., Jr.; Evanseck, J. D.; Field, M. J.; Fischer, S.; Gao, J.; Guo, H.; Ha, S.; Joseph-McCarthy, D.; Kuchnir, L.; Kuczera, K.; Lau, F. T. K.; Mattos, C.; Michnick, S.; Ngo, T.; Nguyen, D. T.; Prodhom, D.; Reiher, W. E., III; Roux, B.; Schlenkrich, M.; Smith, J. C.; Stote, R.; Straub, J.; Watanabe, M.; Wiórkiewicz-Kuczera, J.; Yin, D.; Karplus, M. *J. Phys. Chem. B* **1998**, *102*, 3586.

(38) Halgren, T. A. *J. Comput. Chem.* **1999**, *20*, 730.

(39) Schuler, L. D.; Daura, X.; van Gunsteren, W. F. *J. Comput. Chem.* **2001**, *22*, 1205.

(40) Ponder, J. W.; Case, D. A. *Adv. Prot. Chem.* **2003**, *66*, 27.

(41) MacKerell, A. D., Jr. *J. Comput. Chem.* **2004**, *25*, 1584.

(42) Jorgensen, W. L.; Tirado-Rives, J. *Proc. Natl. Acad. Sci. U.S.A.* **2005**, *102*, 6665.

(43) Landis, C. R.; Root, D. M.; Cleveland, T. *Rev. Comput. Chem.* **1995**, *6*, 73.

(44) Deeth, R. J. *Coord. Chem. Rev.* **2001**, *212*, 11.

(45) Jasper, A. W.; Schultz, N. E.; Truhlar, D. G. *J. Chem. Theory Comput.* **2007**, *3*, 210.

(46) Bhatt, D.; Jasper, A. W.; Schultz, N. E.; Siepmann, J. I.; Truhlar, D. G. *J. Am. Chem. Soc.* **2006**, *128*, 4224.

(47) Bhatt, D.; Schultz, N. E.; Jasper, A. W.; Siepmann, J. I.; Truhlar, D. G. *J. Phys. Chem. B* **2006**, *110*, 26135.

(48) Li, Z. H.; Jasper, A. W.; Truhlar, D. G. *J. Am. Chem. Soc.* **2007**, *129*, 14899.

(49) Li, Z. H.; Bhatt, D.; Schultz, N. E.; Siepmann, J. I.; Truhlar, D. G. *J. Phys. Chem. C* **2007**, *111*, 16227.

(50) Li, Z. H.; Truhlar, D. G. *J. Phys. Chem. C* **2008**, *112*, 11109.

(51) Li, Z. H.; Truhlar, D. G. *J. Am. Chem. Soc.* **2008**, *130*, 12698.

(52) Züttel, A. *Naturwissenschaften* **2004**, *91*, 157.

(53) Pranevicius, L.; Milcius, D.; Pranevicius, L. L.; Thomas, G. *J. Alloys Compd.* **2004**, *373*, 9.

(54) Hayden, L. E.; Tverberg, J. C. *Am. Soc. Mech. Eng. PVP Div.* **2004**, *475*, 223.

(55) Sandrock, G.; Reilly, J.; Graetz, J.; Zhou, W. M.; Johnson, J.; Wegrzyn, J. *Appl. Phys., A* **2005**, *80*, 687.

(56) Yarovsky, I.; Goldberg, A. *Mol. Sim.* **2005**, *31*, 475.

(57) Milcius, D.; Pranevicius, L. L.; Templier, C. *J. Alloys Compd.* **2005**, *398*, 203.

(58) Fichtner, M. *Ann. Chim. Sci. Mater.* **2005**, *30*, 483.

(59) Wagemans, R. W. P.; van Lenthe, J. H.; de Jongh, P. E.; van Dillen, A. J.; de Jong, K. P. *J. Am. Chem. Soc.* **2005**, *127*, 16675.

(60) Graetz, J.; Reilly, J. J. *J. Alloys Compd.* **2006**, *424*, 262.

(61) Graetz, J.; Reilly, J. J. *Scipta Mater.* **2007**, *56*, 835.

(62) Wang, Y.; Yan, J.-A.; Chou, M. Y. *Phys. Rev. B* **2008**, *77*, 014101.

(63) Scheicher, R. H.; Kim, D. Y.; Lebegue, S.; Arnaud, B.; Alouani, M.; Ahuja, R. *Appl. Phys. Lett.* **2008**, *92*, 201903.

(64) Gillespie, R. J. *Chem. Soc. Rev.* **1992**, *21*, 59.

(65) Gilheany, D. G. *Chem. Rev.* **1994**, *94*, 1339.

(66) Albright, T. A.; Burdett, J. K.; Whangbo, M.-H. *Orbital Interactions in Chemistry*; Wiley: New York, NY, 1985.

(67) Hurley, A. C.; Lennard-Jones, J.; Pople, J. A. *Proc. R. Soc. London, Ser. A* **1953**, *220*, 446.

(68) Raff, L. M.; Stivers, L.; Porter, R. N.; Thompson, D. L.; Sims, L. B. *J. Chem. Phys.* **1970**, *52*, 3449.

(69) Hiberty, P. C. *THEOCHEM* **1998**, *451*, 237.

(70) Shaik, S.; Shurki, A. *Angew. Chem., Int. Ed.* **1999**, *38*, 586.

(71) Truhlar, D. G. *J. Comput. Chem.* **2007**, *28*, 73.

(72) Åqvist, J.; Warshel, A. *Chem. Rev.* **1993**, *93*, 2523.

(73) Albu, T. V.; Corchado, J. C.; Truhlar, D. G. *J. Phys. Chem. A* **2001**, *105*, 8465.

(74) Slater, J. C.; Koster, G. F. *Phys. Rev.* **1954**, *94*, 1498.

(75) Hoffmann, R. *J. Chem. Phys.* **1963**, *39*, 1397.

(76) Sutton, A. P.; Finnis, M. W.; Pettifor, D. G.; Ohta, Y. *J. Phys. C* **1988**, *21*, 35.

(77) Foulkes, W. M. C.; Haydock, R. *Phys. Rev. B* **1989**, *39*, 12520.

(78) Porezag, D.; Frauenhein, T.; Köhler, T.; Seifert, G.; Kaschner, R. *Phys. Rev. B* **1995**, *51*, 12947.

(79) Horsfield, A. P. *Phys. Rev. B* **1997**, *56*, 6594.

(80) Harris, J. *Phys. Rev. B* **1985**, *31*, 1770.

(81) Sankey, O.; Niklewski, D. *J. Phys. Rev. B* **1989**, *40*, 3979.

(82) Ducastelle, F. In *Computer Simulation in Materials Science*; Meyer, M., Pontikis, V., Eds.; NATO ASI SeriesE 205: Dordrecht, 1991; p 223.

(83) Lathiotakis, N. N.; Andriotis, A. N.; Mennon, M.; Connolly, J. *J. Chem. Phys.* **1996**, *104*, 992.

(84) Sutton, A. P.; Godwin, P. D.; Horsfield, A. P. *MRS Bull.* **1996**, *21*, 42.

(85) (a) Mehl, M.; Papaconstantopoulos, D. A. *Phys. Rev. B* **1996**, *54*, 4519. (b) Papaconstantopoulos, D. A.; Mehl, M. J. *J. Phys.: Condens. Matter* **2003**, *15*, R413.

(86) (a) Wang, C. Z.; Ho, K. M. *Adv. Chem. Phys.* **1996**, *93*, 651. *Tight-Binding Approach to Computational Materials Science*; (b) Turchi, P. E. A., Gonis, A., Colombo, L., Eds.; Materials Research Society: Warendale, PA, 1998.

(87) Stott, M. J.; Zaremba, E. *Phys. Rev. B* **1980**, *22*, 1564.

(88) Gupta, R. P. *Phys. Rev. B* **1981**, *23*, 6265.

(89) Daw, M. S.; Baskes, M. I. *Phys. Rev. B* **1984**, *29*, 6443.

(90) (a) Baskes, M. *Phys. Rev. B* **1992**, *46*, 2727. (b) Lee, B.-J.; Shim, J.-H.; Baskes, M. I. *Phys. Rev. B* **2003**, *68*, 144112.

(91) (a) Lee, B.-J.; Baskes, M. I.; Kim, H.; Cho, Y. K. *Phys. Rev. B* **2001**, *64*, 184102. (b) Lee, B.-J.; Lee, J. W. *Comput. Coupl. Phase Diagr. Thermochem.* **2005**, *29*, 7.

(92) Finnis, M. W.; Sinclair, J. E. *Phil. Mag. A* **1984**, *50*, 45.

(93) Jacobsen, K. W.; Nørskov, J. K.; Puska, M. J. *Phys. Rev. B* **1987**, *35*, 7423.

(94) (a) Horfield, A. P.; Bratkovsky, A. M.; Fearn, M.; Pettifor, D. G.; Aoki, M. *Phys. Rev. B* **1996**, *53*, 12694. (b) Pettifor, D. G.; Oleinik, I. I. *Phys. Rev. B* **1999**, *59*, 8487. (c) Drautz, R.; Murdick, D. A.; Nguyen-Manh, D.; Zhou, X.; Wadley, H. N. G.; Pettifor, D. G. *Phys. Rev. B* **2005**, *72*, 144105. (d) Aoki, M.; Nguyen-Manh, D.; Pettifor, D. G.; Vitek, V. *Progr. Mat. Sci.* **2007**, *52*, 154.

(95) Stokbro, K.; Jacobsen, K. W. *Phys. Rev. B* **1993**, *47*, 4916.

(96) Polatoglou, H. M.; Methfessel, M.; Scheffler, M. *Phys. Rev. B* **1993**, *48*, 1877.

(97) Rey, C.; Gallego, L. J.; García-Rodeja, J.; Alonso, J. A.; Iñiguez, M. P. *Phys. Rev. B* **1993**, *48*, 8253.

(98) Canel, L. M.; Carlsson, A. E.; Fedders, P. A. *Phys. Rev. B* **1993**, *48*, 10739.

(99) Nastar, M.; Willaime, F. *Phys. Rev. B* **1995**, *51*, 6896.

(100) Foiles, S. M. *MRS Bull.* **1996**, *21*, 24.

(101) Kallinteris, G. C.; Papanicolaou, N. I.; Evangelakis, G. A.; Papaconstantopoulos, D. A. *Phys. Rev. B* **1997**, *55*, 2150.

(102) Garzón, I. L.; Michaelian, K.; Beltrán, M. R.; Posada-Amarillas, A.; Ordejón, P.; Artacho, E.; Sánchez-Portal, D.; Soler, J. M. *Eur. Phys. J. D* **1999**, *9*, 211.

(103) Berthier, F.; Legrand, B.; Tréglia, G. *Interface Sci.* **2000**, *8*, 55.

(104) (a) Karolewski, M. A. *Radiat. Eff. Defects Solids* **2001**, *153*, 239. (b) Mottet, C.; Tréglia, G.; Legrand, B. *Phys. Rev. B* **2002**, *66*, 045413.

(105) Pettifor, D. G.; Aoki, M. In *Equilibrium Structure and Properties of Surfaces and Interfaces*; Gonis, A., Stocks, G. M., Eds.; Plenum Press: New York, 1992; p 123.

(106) (a) Abel, G. C. *Phys. Rev. B* **1985**, *31*, 1985. (b) Tersoff, J. *Phys. Rev. B* **1989**, *39*, 5566.

(107) (a) Brenner, D. W. *Phys. Rev. Lett.* **1989**, *63*, 1022. (b) Brenner, D. W.; Shenderova, O. A.; Shall, J. D.; Areshkin, D. A.; Adiga, S.; Harrison, J. A.; Stuart, S. J. In *Handbook of Nanoscience, Engineering, and Technology*; Goddard, W. A., III; Brenner, D. W., Lyshevski, S. E., IafrateG. J., Eds.; CRC Press: Boca Raton, FL, 2003; p 24.

(108) Baskes, M. I. *Phys. Rev. Lett.* **1987**, *59*, 2666.

(109) (a) London, F. *Z. Elektrochem.* **1929**, *35*, 551. (b) Raff, L. M.; Stivers, L.; Porter, R. N.; Thompson, D. L.; Sims, L. B. *J. Chem. Phys.* **1970**, *52*, 3449. (c) Parr, C. A.; Truhlar, D. G. *J. Phys. Chem.* **1971**, *75*, 1844.

(110) Ackland, G. J.; Reed, S. K. *Phys. Rev. B* **2003**, *67*, 174108.

(111) Morse, P. M. *Phys. Rev.* **1929**, *34*, 57.

(112) (a) Pauling, L. *The Nature of the Chemical Bond*, 3rd. ed.; Cornell University Press: Ithaca, NY, 1960, p 98. (b) Johnston, H. S. *Adv. Chem. Phys.* **1960**, *3*, 131. (c) Lagana, A.; Aspuru, G. O. d.; Garcia, E. *J. Chem. Phys.* **1998**, *108*, 3886. (d) Lendvay, G. *THEOCHEM* **2000**, *501*−*502*, 389.

(113) Hall, G. G. *Theor. Chim. Acta* **1985**, *67*, 439.

(114) (a) Perdew, J. P.; Burke, K.; Ernzerhof, M. *Phys. Rev. Lett.* **1996**, *77*, 3865. (b) Adamo, C.; Barone, V.*J. Chem. Phys.* **1999**, *110*, 6158.

(115) Krishnan, R.; Binkley, J. S.; Seeger, R.; Pople, J. A. *J. Chem. Phys.* **1980**, *72*, 650.

(116) McLean, A. D.; Chandler, G. S. *J. Chem. Phys.* **1980**, *72*, 5639.

(117) Schultz, N. E.; Truhlar, D. G. *J. Chem. Theory Comput.* **2005**, *1*, 41.

(118) Schultz, N. E.; Staszewska, G.; Staszewski, P.; Truhlar, D. G. *J. Phys. Chem. B* **2004**, *108*, 4850.

(119) Kołos, W.; Wolniewicz, L. *J. Chem. Phys.* **1965**, *43*, 2429.

(120) Boothroyd, A. I.; Keogh, W. J.; Martin, P. G.; Peterson, M. R. *J. Chem. Phys.* **1996**, *104*, 7139.

(121) Boothroyd, A. I.; Martin, P. G.; Keogh, W. J.; Peterson, M. J. *J. Chem. Phys.* **2002**, *116*, 666.

(122) Pople, J. A.; Nesbet, R. K. *J. Chem. Phys.* **1954**, *22*, 571.

(123) Dunning, T. H., Jr. *J. Chem. Phys.* **1989**, *90*, 1007.

(124) Brown, F. B.; Shavitt, I.; Shepard, R. *Chem. Phys. Lett.* **1984**, *105*, 363.

(125) Pople, J. A.; Seeger, R.; Krishnan, R. *Int. J. Quantum Chem. Symp* **1977**, *11*, 149.

(126) Roos, B. O.; Taylor, P. R.; Siegbahn, P. E. M. *Chem. Phys.* **1980**, *48*, 157.

(127) Ruedenberg, K.; Schmidt, M. W.; Gilbert, M. M.; Elbert, S. T. *Chem. Phys.* **1982**, *71*, 41.

(128) Truhlar, D. G. *Chem. Phys. Lett.* **1998**, *294*, 45.

(129) Carroll, D. L. In *Developments in Theoretical and Applied Mechanics*; Wilson, H., Batara, R., Bert, C., Davis, A., Schapery, R., Stewart, D., Swinson, F., Eds.; School of Engineering, The University of Alabama: Tuscaloosa, AL, 1996; Vol. 17, p 411.

(130) Carroll, D. L. *GA-version 1.7a: FORTRAN Genetic Algorithm Driver*; CU Aerospace: Urbana, IL, 2001.

(131) Message Passing Interface Forum. *Document for a standard message passing interface, Technical Report No. CS-93-214*; University of Tennessee: Knoxville, TN, 1994.

(132) Gropp, W.; Lusk, E.; Skjellum, A. *Using MPI: Portable Parallel Programming with the Message-Passing Interface*; 2nd ed.; MIT Press: Cambridge, MA, 1999.

(133) Davidson, E. R. *Chem. Rev.* **1993**, *93*, 2337.

(134) Baskes, M. I.; Nelson, J. S.; Wright, A. F. *Phys. Rev. B* **1989**, *40*, 6085.

(135) Vashishta, P.; Kalia, R. K.; Nakano, A. *J. Phys. Chem. B* **2006**, *110*, 3727.

(136) Kadai, K.; Germann, T. C.; Lomdahl, P. S.; Albers, R. C.; Wark, J. S.; Higgenbotham, A.; Holian, B. L. *Phys. Rev. Lett.* **2007**, *98*, 135701.

(137) Gonzalez-Lafont, A.; Truong, T. N.; Truhlar, D. G. *J. Phys. Chem.* **1991**, *95*, 4618.

(138) Rossi, I.; Truhlar, D. G. *Chem. Phys. Lett.* **1995**, *233*, 231.

(139) Bash, P. A.; Ho, L. L. jr.; Levine, D.; Hallstrom, P. *Proc. Natl. Acad. Sci. USA* **1996**, *93*, 3698.

(140) Layfield, J. P.; Owens, M. D.; Troya, D. *J. Chem. Phys.* **2008**, *128*, 194302.

CT8004535